Materials Research Express

PAPER

Effect of B or N doping on the dielectric and electrical properties of ZnO at room temperature

To cite this article: Ali Can Güler *et al* 2019 *Mater. Res. Express* **6** 065017

Materials Research Express

RECEIVED
24 December 2018

REVISED
12 February 2019

ACCEPTED FOR PUBLICATION
28 February 2019

PUBLISHED
15 March 2019

PAPER

Effect of B or N doping on the dielectric and electrical properties of ZnO at room temperature

Ali Can Güler[1], **Bircan Dindar**[1,2,4] and **Hümeyra Örücü**[3]

[1] Material Science and Engineering Department, Ege University, 35100, Bornova, İzmir, Turkey
[2] Solar Energy Institute, Ege University, 35100, Bornova, İzmir, Turkey
[3] Faculty of Science, Physics Department, Ege University, 35100, Bornova, İzmir, Turkey
[4] Author to whom any correspondence should be addressed.

E-mail: alican-guler@hotmail.com, bbdindar@yahoo.com, bircan.dindar@ege.edu.tr and humeyra.orucu@ege.edu.tr

Keywords: dielectric properties, mechanochemical synthesis, B doped ZnO, N doped ZnO, capacitance

Supplementary material for this article is available online

Abstract

Boron (B) or nitrogen (N) doped ZnO nanoparticles were fabricated using mechanochemical technique. To research the effect of doping rate on the dielectric and electrical properties, B_n-ZnO and N_n-ZnO (n = 2 and 4 wt%) were obtained. The chemical compositions of the produced metal oxides were determined by Fourier transform infrared spectroscopy (FTIR). Several vibration modes caused by specific substituents were observed for all samples in FTIR spectra. The dielectric spectra were also analysed in the light of earlier results for an elaborative examination. Dielectric behaviours of the undoped and B or N doped ZnO nanostructures were studied by means of dielectric spectroscopy (DS) in the large frequency range 10^{-2}–10^{7} Hz at room temperature. As a result of the dielectric study of ZnO with B or N dopants, remarkable changes in dynamics such as dielectric constant, dielectric loss tangent, capacitance and electrical conductivity were obtained in tune with Koop's theory. The electrical conductivity response for the entire samples obeyed the Jonscher power law equation, and the hopping mechanism between ionized oxygen vacancies was found to dominate the conduction mechanisms in the undoped and doped ZnO nanoparticles. The maximum dielectric constant in this study (60 at 1 Hz) has been achieved with the N doped ZnO samples. It was also determined that N doping increased the undoped ZnO capacitance value from 5.14×10^{-11} F to 2.64×10^{-10} F, whereas B doping decreased it up to 1.56×10^{-11} F.

1. Introduction

In the development of many cutting edge technologies, mainly electronic and optoelectronic, fabrication of semiconductor nanoparticles and determining their material properties are of utmost importance. Zinc oxide (ZnO) is one of technologically promising material that possesses controllable intrinsic n-type conductivity, a wide direct band gap (Eg $\approx$ 3.37 eV) and large excitonic binding energy (60 meV) at room temperature [1, 2]. ZnO crystallizes in wurtzite type, comprising of tetrahedral structures in which a Zn atom is surrounded by four O atoms, and vice versa. The noncentrosymmetric tetrahedral structure of ZnO induces piezoelectric properties, crystallographic polarity and defects [3]. Multifunctionality of ZnO is also remarkable for applications of dielectrics. Capacitors, microwave telecommunications, satellite broadcasting and non-volatile memory device applications require materials with low and high dielectric constants and low dielectric loss [4].

It is widely-recognized that electrical and dielectric properties of semiconductors are significantly influenced by doping appropriate impurity atoms. Many studies have been reported on the manipulated dielectric properties of ZnO doped with a variety of elements, predominantly metals [5–7]. Recently, Das *et al* obtained a high dielectric constant of 1.2×10^{6} due to the grain boundary defects caused by Gd and Mn doping in ZnO [8]. A significant increase in dielectric constant and decrease in dielectric loss were observed as a result of Al incorporation into ZnO lattice [9]. R. Saravanan *et al* found that transition metal doping enhanced DC

conductivity of ZnO while reducing the energy dissipation [10]. Furthermore, Jayachandraiah and Krishnaiah proposed that frequency dependent dielectric constant, dielectric loss tangent and electrical conductivity properties were decreased with Er doping [11].

In the past, B and N elements have been employed several times to modify electrical and optical properties of ZnO thin films [12–15]. Senol *et al* found that electrical resistivity of the ZnO nanopowders decreased from 10.89×10^4 Ω.cm to 1.25×10^4 Ω.cm with increase of B doping concentrations at room temperature [16]. Moreover, Xiaming showed that N doped ZnO thin films can be used as active channel layer in field effect transistors (FET) [17]. Consequently, the lack of the dielectric study of ZnO using B or N dopants has motivated us to carry out this report. So far, various synthesis methods such as sol-gel, chemical vapor deposition, chemical spray pyrolysis, hydrothermal, solvothermal, microwave assisted and mechanochemical processes were applied for producing B or N doped ZnO nanostructures and thin films [18–23]. The cost-effective and easy mechanochemical technique stands out among all processes in that it facilitates the production of separated nanoparticles [24].

In this research paper, investigation on the dielectric and electrical properties of B or N doped ZnO nanoparticles (2 and 4 wt%) synthesized through solid mechanochemical technique is discussed. After fabrication, the chemical composition and dielectric characteristics of the samples were enlightened using Fourier transform infrared spectroscopy (FTIR) and dielectric spectroscopy (DS), respectively. The structural, morphological and optical characterization of the synthesized undoped and B or N doped ZnO samples were earlier performed with x-ray diffractometer (XRD), x-ray photoelectron spectroscopy (XPS), scanning electron microscope (SEM), energy dispersive spectroscopy (EDS), atomic force microscopy (AFM), photoluminescence spectroscopy (PL) and UV–vis diffuse reflectance spectrophotometer (DRS), and the experimental results were discussed in detail in our previous work [25]. Furthermore, exploring the effects of B or N dopant and their concenrations on frequency dependent dielectric constant, capacitance, dielectric loss tangent and electrical conductivity of ZnO were accomplished in this study.

2. Experimental

2.1. Chemicals

Zinc acetate dihydrate [Sigma-Aldrich, $Zn(CH_3CO_2)_2.(H_2O)_2$], oxalic acid [Merck, $(C_2H_2O_4)$], boric acid [Horasan, (H_3BO_3)] and urea [Merck, (CH_4N_2O)], KBr [Merck] were purchased and used as received without any further purification.

2.2. Characterization

The influences of doping element type and amount of them on electrical and dielectric properties of zinc oxide nanoparticles were investigated using dielectric spectroscopy (DS, Novocontrol BDS 80 High-Resolution Broadband Dielectric Spectrometer) in a frequency range 10^{-2}–10^7 Hz at room temperature. For the DS measurements, the powder samples were pressed into cylindrical pellets of 10 mm diameter and 0.55 mm thickness. The chemical composition of the samples was determined employing Fourier transform infrared spectroscopy (FTIR, Perkin Elmer Spectrum BX). All synthesized ZnO samples were prepared as transparent pellets in a 10 mm diameter by mixing 1% in KBr medium for FTIR analyses.

2.3. Synthesis of materials

To determine the dielectric and electrical properties, the undoped ZnO and B or N doped ZnO nanopowders were synthesized in a similar manner to our previous work, as shown in scheme 1. A bowl-like mortar was used to grind substances. At the beginning, 2.195 g zinc acetate dihydrate and 1.512 g oxalic acid were placed in the mortar and ground for 10 min. After the first grinding process, boric acid was put into this pot as boron source and crushing the mixture was proceeded for another 10 min. Following this, the paste mixture was calcined at 500 °C for 3 h. N doped ZnO samples were prepared with the same procedure using urea as nitrogen source. ZnO doped with 2 and 4 wt% of B or N were synthesized to understand the effect of the doping amount on the dielectric properties. The pure ZnO was also synthesized without the addition of boric acid or urea under the same conditions to be able to make a comparison.

3. Result and discussion

3.1. Structural and morphological properties

It is necessary to emphasize the pre-measured characteristic properties of B or N doped ZnO materials again. The XRD patterns of the synthesized nanostructures were attributed to hexagonal wurtzite structure. It is evident from XPS and EDS spectra that the obtained samples are only composed of Zn, O, N or B elements,

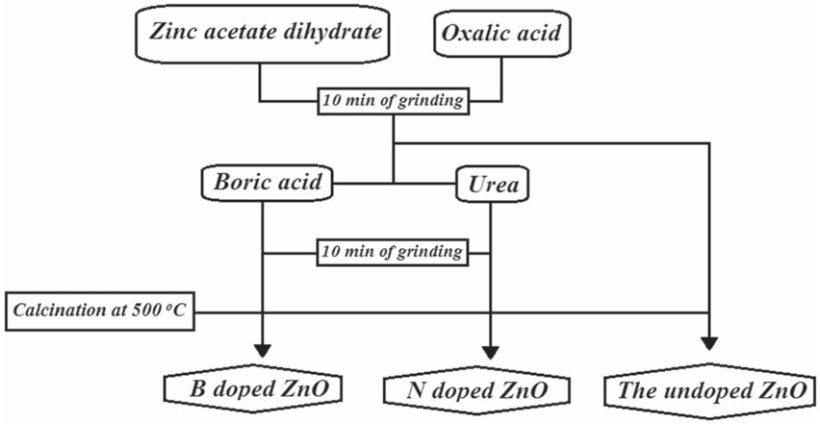

Scheme 1. Flow chart for the mechanochemical processing of the undoped, B doped and N doped ZnO powder samples.

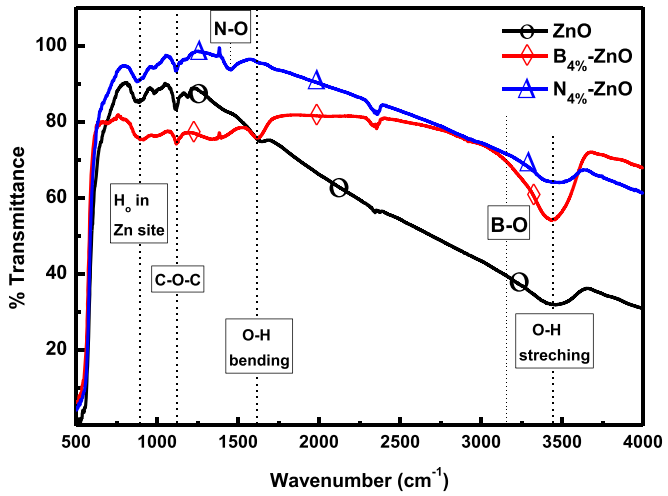

Figure 1. FTIR spectra of the undoped ZnO, $B_{4\%}$-ZnO and $N_{4\%}$-ZnO.

indicating high purity. 3D AFM images represented that the incorporation of B or N impurity atoms into ZnO increased its roughness value and led to higher surface porosity. In the SEM images of the undoped and N doped ZnO samples, 'rod-like' hexagonal crystals are predominant in the agglomeration of particles, whereas cubic structure dominates B doped ZnO. It is observed that the near UV emission bands appeared in PL spectra for the all samples were associated with the exciton recombination, and the optical band gaps of the samples were found to be in the range of 3.38–3.48 eV [25].

Fourier transform infrared spectroscopy (FTIR) was used to identify the chemical composition of the samples. Figure 1 illustrates the FTIR spectra of the undoped ZnO and 4 wt% B or N doped ZnO nanostructures calcined at 500 °C for 3 h. All samples exhibited several vibration modes caused by specific substituents. The broad peaks appearing at 3439–3457 cm^{-1} and 1625–1643 cm^{-1} are consistent with the literature, and corresponding to O-H stretching and O-H bending modes of hydroxyl groups of absorbed water, respectively [26]. The tiny peaks observed at 1116–1190 cm^{-1} were attributed to C-O-C stretching modes of acetate species, which can exist on the material surface [27, 28]. According to Kumari *et al*, the vibrational modes ~885 cm^{-1} are originated from the substitutional hydrogen (H_o) at oxygen site bound to the lattice Zn location, which may act as donor state in ZnO [29]. It is also noteworthy that the small peak widening at 3200–3250 cm^{-1} for B doped ZnO and the peak at 1450–1500 cm^{-1} for N doped ZnO are due to B-O bond of boron oxide and N-O bond of N doped ZnO, respectively [30].

3.2. Electrical and dielectric properties

Dielectric spectroscopy (DS) is a very effective tool for determining the dielectric behaviour of solid materials by providing a non-destructive investigation advantage. In this section, dynamic properties like dielectric constant,

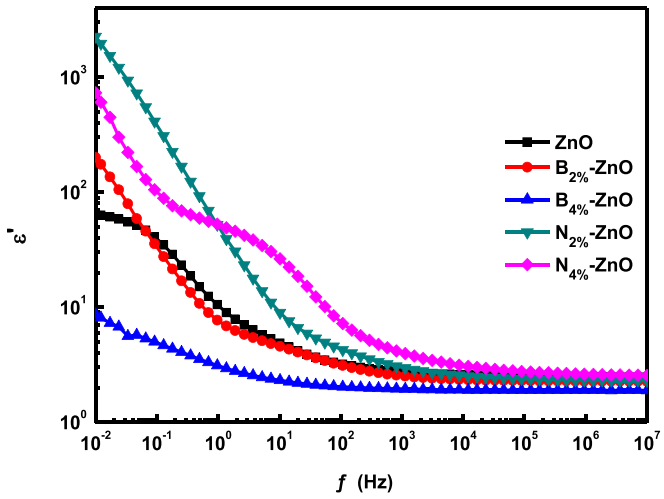

Figure 2. Variation of dielectric constant of the undoped and B or N doped ZnO nanopowders.

dielectric loss, electrical conductivity and capacitance of the undoped and B or N doped ZnO samples were discussed in a wide frequency range 10^{-2}–10^{7} Hz at room temperature.

3.2.1. Dielectric constant

Dielectric dispersion of solid materials is often explained by expression of the complex relative dielectric constant, which consists of a real part (ε') and an imaginary part (ε'')

$$\varepsilon^* = \varepsilon' + j\,\varepsilon'' \tag{1}$$

The real part is a measure of the amount of energy stored from the applied electric field in the material, whereas the imaginary part describes the energy loss (dissipation energy). The real part of dielectric constant can be calculated by the correlation

$$\varepsilon' = \frac{Cd}{A\varepsilon_o} \tag{2}$$

C is capacitance, d and A, respectively, are thickness and cross-sectional area of the pellet samples and ε_0 is permittivity of the free space (8.85×10^{-12} F m^{-1}).

The variation of dielectric constant with frequency for the undoped and B or N doped ZnO nanoparticles are shown in figure 2. It is clearly seen that dielectric constant values decrease rapidly in low frequency region and become almost frequency independent at higher frequency region for the entire samples. After a certain point at low frequency region, the dipole moment cannot follow the fast-changing applied electric field, and being not able to contribute to the net polarization anymore leads to a decrease in dielectric constant. Therefore, there is a decrement in dielectric constant values of the samples with increasing frequency. This type of dielectric behaviour is common reported trend of n-type ZnO nanostructures, and can be explained based upon the Koop's theory. In this model, dielectric materials are postulated to be composed of dielectric boundary layers of Maxwell-Wagner type in which grains with low dielectric constant value are divided by grain boundaries with high dielectric constant value [31].

The dielectric constant of N doped ZnO is explicitly higher compared to that of the undoped ZnO, on the contrary, the increasing amount of B doping attenuates dielectric constant of ZnO. A literature compatible dielectric constant of the undoped ZnO was obtained about 10 at 1 Hz [32]. The maximum dielectric constant at 1 Hz (60) has been achieved with N doped ZnO samples. The space charge polarization and orientation polarization are two major dielectric polarization mechanisms in ZnO. The former is dominant in low frequency region, and the latter is dominant in high frequency region. For ZnO nanostructures, there can exist large amount of structural defects such as vacancies and dangling bonds by doping with different size ions in comparison with Zn and O as well as synthesis process [9]. The charge carriers generated upon the incorporation of dopant ions into ZnO can easily travel and accumulate in the edge of grain boundaries are likely to be trapped in defects described above, and result in the formation of electric dipoles cause space charge polarization. The PL spectra suggests that N doped ZnO has higher PL intensity and B doped ZnO has lower PL intensity according to that of ZnO. A high PL intensity refers to high electron-hole recombination rate and less free charge carrier concetration. Therefore, the high dielectric constant by N doping and low dielectric constant by B doping were respectively attributed to the rise and fall in amount of free charge carriers. These charge carriers segregate at

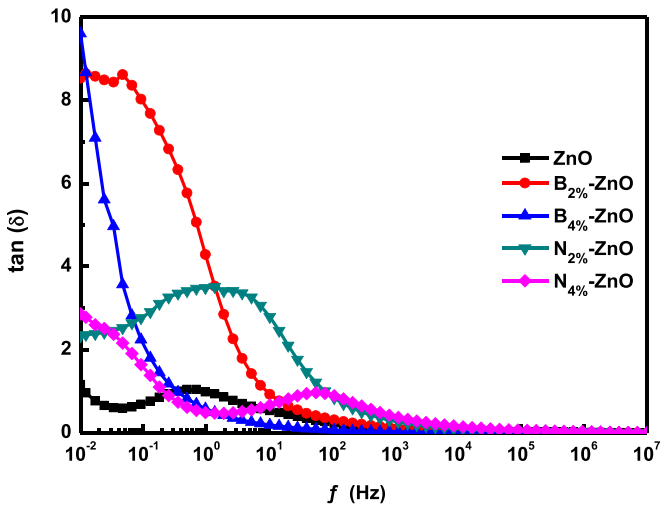

Figure 3. Variation of dielectric loss tangent of the undoped and B or N doped ZnO nanopowders.

grains and account for space charge polarization in low frequencies. On the other hand, plenty of the negative oxygen vacancies (O^{-2}) and the positive zinc interstitials (Zn^{+2}) exchanging their positions in close atomic neighbourhoods are thought to be possible sources of orientation polarization in high frequencies [33]. In the PL spectra, no emission peaks associated to the imperfections or impurities were observed, however, the calculated activation energy confirms the existence of oxygen vacancies along the zinc interstitial-acceptor complexes that are involved in hopping mechanism.

The crystallite size of the undoped, N doped and B doped ZnO were calculated to be 17, 16 and 8 nm, respectively. Referring to the dielectric constant, the values have decreasing tendency with decreasing crystallite size in contrast to surface energy. The large surface energy can produce large grain growth rate. That is to say, the smaller crystallite size triggers the formation of large grains in the sample. Thus, the grain size of B doped ZnO is expected to be larger than those of the undoped ZnO and N doped ZnO nanoparticles. The large grain structure of B doped ZnO signifies smaller number of grains or amount of grain boundaries, and in turn it explains the decrease in dielectric constant. Das *et al* have also reported that dielectric constant is bound up with the number of grains or amount of effective grain boundaries [7].

3.2.2. Dielectric loss tangent

Dielectric loss tangent or loss factor (tan δ) is a quantity representing the energy dissipation (as heat) in a dielectric material that can be calculated using the relation

$$\tan \delta = \varepsilon''/\varepsilon' \tag{3}$$

The variation of dielectric loss tangent at room temperature as a function of frequency for all samples were illustrated in figure 3. Dielectric loss tangent is subject to electrical conductivity, and naturally to the number of charge carriers in the material. Unusual peaks were displayed in dielectric loss tangent spectra of the undoped and N doped ZnO samples,. The peaks appearing were assigned to the presence of relaxing dipoles and the resonance effect, which occurs in the case that the hopping frequency of localised charge carriers equals to frequency of the applied electric field [33, 34].

Another observation in the dielectric loss tangent plot is peak shifting with higher N doping. Singh *et al* have shown that a peak shifted to higher frequencies are owing to the increased number of relaxing dipoles, and leads to increase in electrical conductivity [35]. Therefore, it can be concluded that N incorporated into ZnO acting as acceptor impurities enhanced the number of free charge carriers and the number of electric dipoles contributing to polarization. In addition to that dielectric loss tangent of B doped ZnO samples was found to be decreasing with the increase in frequency as well as rising in the amount of B dopant. It is reasonably thought that ZnO nanoparticles doped with B have the potential to be used in high frequency applications.

3.2.3. Dielectric relaxation time

Relaxation is typically the time-dependent recovery of strain on removal of stress, analogously to dielectric relaxation in response to an applied electric field. Despite the individual characteristic time for a given dipole, in a statistical case, there is an average value which is the relaxation time of the dielectric system. The dielectric relaxation time (τ) is defined as the moment that polarization is exponentially reduced to its original value at a

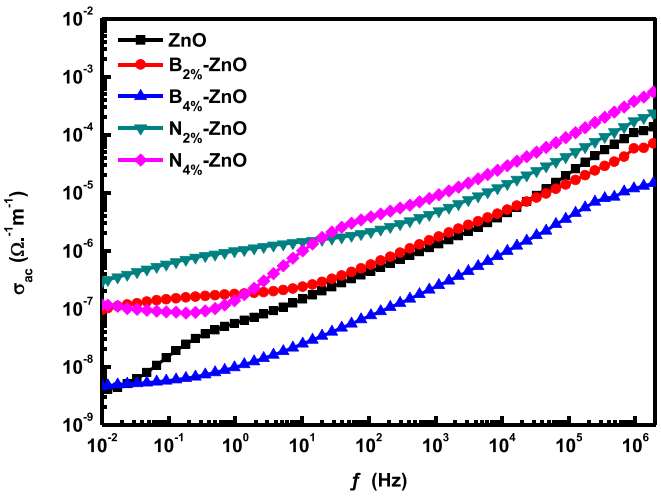

Figure 4. Variation of ac conductivity of the undoped and B or N doped ZnO nanopowders.

certain frequency. This dielectric relaxation frequency ($f_{\tan\delta}$) corresponds to the maximum value of dielectric loss tangent. The dielectric relaxation time of the samples were evaluated from the resonance condition $2\pi f_{\tan\delta}\tau = 1$. Relaxation frequency varies with the population of defects and the temperature. Therefore, room temperature analysing facilitates to investigate only the effect of doping on dielectric relaxation [10, 35].

3.2.4. Electrical conductivity

The total electrical conductivity (σ_{tot}) is the sum of the dc conductivity (σ_{dc}) and the ac conductivity (σ_{ac}). The following equation can obtain the ac conductivity,

$$\sigma_{ac} = \varepsilon'\varepsilon_0\omega \tan\delta \tag{4}$$

Where Ω is the angular frequency ($\Omega = 2\pi f$). The variation of the ac conductivity with frequency of the undoped and B or N doped ZnO pellets are depicted in figure 4. The conductivities were analysed considering Jonscher power law equation

$$\sigma = \sigma_{dc} + A\omega^n \tag{5}$$

Where σ_{dc} is the DC conductivity, A is the constant and n is the frequency dependent exponent.

Figure 5 shows the logarithmic plots of the ac conductivity versus the angular frequency at which the exponent values have been accurately calculated from the slope. The n exponent values of the samples are in the range of 0.32–0.52. According to the power law, the exponent varying between 0 and 1 implies that the conduction mechanism is frequency dependent. In other words, the exponent confirms the divergence from Debye type relaxation where the exponent n is equivalent to zero [8, 36].

The influence of doping on the DC conductivity, dielectric loss tangent, capacitance and relaxation time is present in table 1. It was also determined that N doping increased the undoped ZnO capacitance value from 5.14×10^{-11} F to 2.64×10^{-10} F, whereas B doping decreased it up to 1.56×10^{-11} Hembram *et al* suggest that the grain boundary capacitance value for ZnO electroceramic materials is generally in the orders of 10^{-11}–10^{-8} F [37].

The explored variation of the ac conductivity for the all specimens is flat-like line at low frequencies and increases linearly through high frequencies with contributions from the dc conductivity and the ac conductivity, respectively. This kind of response refers to localised conduction process in opposition to the free band conduction process. In ZnO semiconductor, hopping of charge carriers between different localised states is the main responsible for the conductivity because the most of the free charge carriers are trapped by point defects again [32, 38]. An activation energy is evidently required for the hopping charge transport mechanism. Pike has developed a model to explain the charge transport mechanism between localised states [39]. According to this model, charge carriers around ionised impurity or outside a vacancy hop over a Coulomb-like potential barrier with W_M activation energy,

$$W_M = W + \left(\frac{4e^2}{\varepsilon R}\right) \tag{6}$$

Where W is the barrier height insulating two sites, ε is the dielectric constant of the medium and R is the distance between localized states. In Pike's model, the exponent n is expressed as

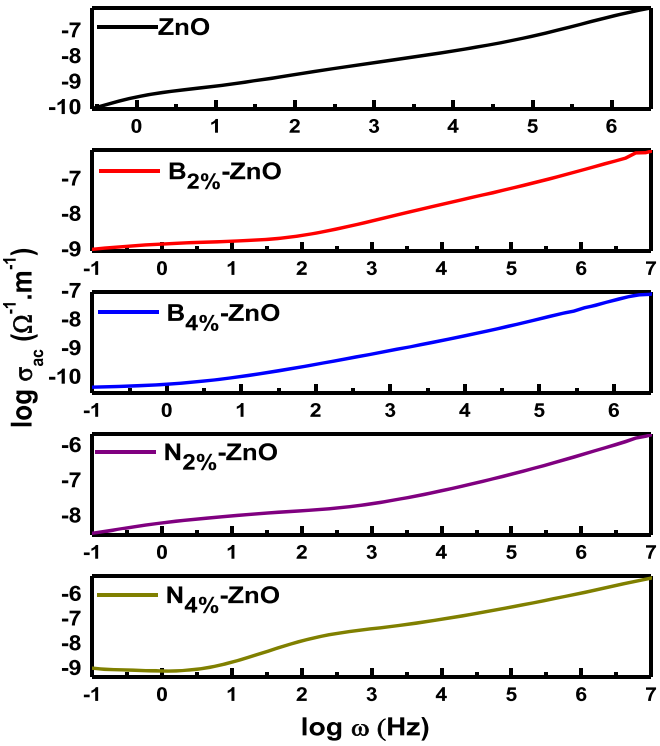

Figure 5. Log σ_{ac} versus log ω plots for the undoped ZnO and $B_{2\%}$, $B_{4\%}$, $N_{2\%}$ and $N_{4\%}$ doped ZnO.

Table 1. Effect of doping on dielectric properties of ZnO nanoparticles.

Sample	τ (ms)	C (F) at 1 Hz	tan δ at 1 Hz	σ_{dc} (Ω^{-1}.m^{-1})
ZnO	2.75×10^{2}	5.14×10^{-11}	0.97	5.23×10^{-9}
$B_{2\%}$-ZnO	3.18×10^{3}	4.10×10^{-11}	4.29	1.30×10^{-7}
$B_{4\%}$-ZnO	1.59×10^{4}	1.56×10^{-11}	0.57	4.85×10^{-9}
$N_{2\%}$-ZnO	1.22×10^{2}	2.39×10^{-10}	3.41	4.75×10^{-7}
$N_{4\%}$-ZnO	2.90×10^{0}	2.64×10^{-10}	0.45	7.87×10^{-8}

$$n = 1 - \frac{6kT}{W_M} \tag{7}$$

Where k is the Boltzmann constant and T is the absolute temperature. The activation energy W_M at room temperature for the undoped ZnO, $B_{4\%}$-ZnO, $N_{4\%}$-ZnO, $B_{2\%}$-ZnO and $N_{2\%}$-ZnO nanopowders were calculated, and found to be 0.32, 0.29, 0.30, 0.24 and 0.23 eV, respectively. It has been shown in few literatures that the activation energy of 0.29 eV is associated with the oxygen vacancy [40]. And although we could not find any information in literature that can literally correspond to activation energies of $B_{2\%}$-ZnO and $N_{2\%}$-ZnO (0.23–0.24 eV), the activation energy of Zn interstitial-acceptor complex (~0.15–0.20 eV) might encounter to them [41, 42]. As noticeable, the hopping mechanisms of %2 and %4 doped samples were predominated with two different ionised states in which the free charge carrier can be trapped again.

In conductivity of the mechanochemically synthesized ZnO, a significant enhancement with higher N doping and derogation with higher B doping have been attained. The increased conductivity of N doped ZnO is ascribed to the extra free charge carriers induced by either N^{3-} ion replacing with O^{2-} ion or occupation of N^{3-} ion in the interstitial sites of ZnO lattice [43]. The better the crystal structure of the material, the intensive and narrower diffraction peaks are obtained, and a better crystal structure contributes more to the electrical conductivity; hence the higher electrical conductivity of N doped ZnO is also elucidated based on its good crystallinity. The XRD response of B doped ZnO exhibits a considerably deteriorated crystallinity, consisting of grains large in size and small amount of grain boundaries. This finding is also in good agreement with SEM and AFM results. Therefore, the decrease in conductivity with B doping might stem from that the defects tend to diffuse at the grain boundary interfaces in sintering and cooling processes. These defects act as potential barriers and retard the flow of free charge carriers in ZnO [11, 44]. In addition, in XPS survey, the presence of inactive

oxides of boron (B_2O_3) in ZnO, having a wide band gap of 6.3 eV could be other possible reason of decrease in the conductivity.

4. Conclusion

In summary, the undoped and B or N doped ZnO nanoparticles have been successfully synthesized using mechanochemical method and characterised by several techniques. In the all dynamic properties of the undoped ZnO, there was an increase with higher N doping and a decrease with higher B doping. Dielectric constant, capacitance and dielectric loss tangent curves were found to be decreasing with increasing frequency of the applied electrical field. Moreover, N doping caused an increase in the capacitance value of the ZnO, whereas B doping has reduced it. According to the dielectric loss tangent spectra, B doped ZnO is a promising candidate to be used in high frequency region. We observed that incorporation of B or N into ZnO crystal generated imperfections such as oxygen vacancies involving in the hopping mechanism. Consequently, B or N doping substantially influenced the electrical and dielectric properties of ZnO nanoparticles and a remarkable enhancement in the conductivity of ZnO was obtained as a result of N doping.

Acknowledgments

We are grateful to Scientific Research Projects Directorate of Ege University for providing financial assistance to this research study (Project No: 16 GEE 010 and 16 FBE 010). We also wish to thank Assoc. Prof Ivo Kuřitka in Tomas Bata University for DS analyses.

ORCID iDs

Ali Can Güler https://orcid.org/0000-0002-3828-0138
Bircan Dindar https://orcid.org/0000-0002-3478-5550

References

[1] Yayapao O, Thongtem T, Phuruangrat A and Thongtem S 2015 Synthesis and characterization of highly efficient Gd doped ZnO photocatalyst irradiated with ultraviolet and visible radiations *Mater. Sci. Semicond. Process.* **39** 786–92
[2] Ba-Abbad M M, Kadhum A A H, Mohamad A B, Takriff M S and Sopian K 2013 Visible light photocatalytic activity of Fe3+-doped ZnO nanoparticle prepared via sol–gel technique *Chemosphere* **91** 1604–11
[3] Samadi M, Zirak M, Naseri A, Khorashadizade E and Moshfegh A Z 2016 Recent progress on doped ZnO nanostructures for visible-light photocatalysis *Thin Solid Films* **605** 2-19
[4] Goel S, Sinha N, Yadav H, Godara S, Joseph A J and Kumar B 2017 Ferroelectric Gd-doped ZnO nanostructures: enhanced dielectric, ferroelectric and piezoelectric properties *Mater. Chem. Phys.* **202** 56–64
[5] Gürbüz O and Okutan M 2016 Structural, electrical, and dielectric properties of Cr doped ZnO thin films: role of Cr concentration *Appl. Surf. Sci.* **387** 1211–8
[6] Wang J, Wang Z, Liu R, Li Y, Zhao X and Zhang X 2017 Heterogeneous interfacial polarization in Fe@ZnO nanocomposites induces high-frequency microwave absorption *Mater. Lett.* **209** 276–9
[7] Das S, Bandyopadhyay A, Das S, Das D and Sutradhar S 2018 Defect induced room-temperature ferromagnetism and enhanced dielectric property in nanocrystalline ZnO co-doped with Tb and Co *J. Alloys Compd.* **731** 591–9
[8] Das S, Das S and Sutradhar S 2017 Enhanced dielectric behavior and ac electrical response in Gd-Mn-ZnO nanoparticles *J. Alloys Compd.* **726** 11–21
[9] Zamiri R, Singh B, Belsley M S and Ferreira J M F 2014 Structural and dielectric properties of Al-doped ZnO nanostructures *Ceram. Int.* **40** 6031–6
[10] Saravanan R, Prakash T, Gupta V K and Stephen A 2014 Tailoring the electrical and dielectric properties of ZnO nanorods by substitution *J. Mol. Liq.* **193** 160–5
[11] Jayachandraiah C and Krishnaiah G 2015 Erbium induced raman studies and dielectric properties of Er-doped ZnO nanoparticles *Adv. Mater. Lett.* **6** 743–8
[12] Bel Hadj Tahar R and Bel Hadj Tahar N 2005 Boron-doped zinc oxide thin films prepared by sol-gel technique *J. Mater. Sci.* **40** 5285–9
[13] Jana S, Vuk A S, Mallick A, Orel B and Biswas P K 2011 Effect of boron doping on optical properties of sol–gel based nanostructured zinc oxide films on glass *Mater. Res. Bull.* **46** 2392–7
[14] Tuzemen E S, Kara K, Elagoz S, Takci D K, Altuntas I and Esen R 2014 Structural and electrical properties of nitrogen-doped ZnO thin films *Appl. Surf. Sci.* **318** 157–63
[15] Lu J, Ye Z, Wang L, Huang J and Zhao B 2003 Structural, electrical and optical properties of N-doped ZnO films synthesized by SS-CVD *Mater. Sci. Semicond. Process.* **5** 491–6
[16] Senol S D, Ozturk O and Terzioğlu C 2015 Effect of boron doping on the structural, optical and electrical properties of ZnO nanoparticles produced by the hydrothermal method *Ceram. Int.* **41** 11194–201
[17] Zhu X, Wu H, Wang S, Zhang Y, Cai C, Si J, Yuan Z, Du X and Dong S 2009 Optical and electrical properties of N-doped ZnO and fabrication of thin-film transistors *J. Semicond.* **3** 1–4
[18] Ilican S, Yakuphanoglu F, Caglar M and Caglar Y 2011 The role of pH and boron doping on the characteristics of sol gel derived ZnO films *J. Alloys Compd.* **509** 5290–4

[19] Yu Q, Li J, Li H, Wang Q, Cheng S and Li L 2012 Fabrication, structure, and photocatalytic activities of boron-doped ZnO nanorods hydrothermally grown on CVD diamond film *Chem. Phys. Lett.* **539–540** 74–8
[20] Pawar B N, Cai G, Ham D, Mane R S, Ganesh T, Ghule A, Sharma R, Jadhava K D and Han S 2009 Preparation of transparent and conducting boron-doped ZnO electrode for its application in dye-sensitized solar cells *Sol. Energy Mater. Sol. Cells* **93** 524–7
[21] Gao S, Jiao S and Lei B 2015 Efficient photocatalyst based on ZnO nanorod arrays/p -type boron-doped-diamond heterojunction *J. Mater. Sci., Mater. Electron.* **26** 1018–22
[22] Zhang D, Gong J, Ma J, Han G and Tong Z 2013 A facile method for synthesis of N-doped ZnO mesoporous nanospheres and enhanced photocatalytic activity *Dalt. Trans.* **42** 16556–61
[23] Gionco C, Fabbri D, Calza P and Paganini M C 2016 Synthesis, characterization, and photocatalytic tests of N-doped zinc oxide: a new interesting photocatalyst *J. Nanomater.* **2016** 1–7
[24] Aghababazadeh R, Mazinani B, Mirhabibi A and Tamizifar M 2006 ZnO Nanoparticles Synthesised by mechanochemical processing *J. Phys.: Conf. Ser.* **26** 312–4
[25] Dindar B and Can A 2018 Environmental nanotechnology, monitoring & management comparison of facile synthesized N doped, B doped and undoped ZnO for the photocatalytic removal of rhodamine B *Environ. Nanotechnology, Monit. Manag.* **10** 457–66
[26] Lamba R, Umar A, Mehta S K and Kansal S K 2015 ZnO doped SnO_2 nanoparticles heterojunction photo-catalyst for environmental remediation *J. Alloys Compd.* **653** 327–33
[27] Bechambi O, Sayadi S and Najjar W 2015 Photocatalytic degradation of bisphenol A in the presence of C-doped ZnO: effect of operational parameters and photodegradation mechanism *J. Ind. Eng. Chem.* **32** 201–10
[28] Barick K C, Singh S, Aslam M and Bahadur D 2010 Porosity and photocatalytic studies of transition metal doped ZnO nanoclusters *Microporous Mesoporous Mater.* **134** 195–202
[29] Kumari R, Sahai A and Goswami N 2015 Effect of nitrogen doping on structural and optical properties of ZnO nanoparticles *Prog. Nat. Sci. Mater. Int.* **25** 300–9
[30] Bozacı E 2018 Borlu bileşiklerin çevre dostu yöntemlerle poliakrilnitril kumaşlara uygulanması *J. Boron* **3** 17–23
[31] Cvejić Ž, Rakić S, Jankov S, Skuban S and Kapor A 2008 Dielectric properties of nanosized ZnFe2O4 *Process. Appl. Ceram.* **2** 53–66
[32] Cheng P-F, Li S-T and Wang H 2013 Dielectric spectroscopy studies of ZnO single crystal *Chinese Phys.* B **22** 1–4
[33] Varshney D, Verma K and Dwivedi S 2015 Structural and dielectric studies of hexagonal ZnO nanoparticles *Opt. - Int. J. Light Electron Opt.* **126** 4232–6
[34] Malyshkina O V, Ivanova A I, Luzin R, Makarenkov I, Pugachev S I and Rytov E 2015 Effect of bismuth oxide dispersivity on the dielectric properties of zinc oxide ceramics *IOP Conf. Ser.: Mater. Sci. Eng.* **77** 1–4
[35] Singh P K, Gaur M S and Chauhan R S 2015 Dielectric properties of sol-gel synthesized polysulfone-ZnO nanocomposites *J. Therm. Anal. Calorim.* **122** 725–40
[36] Jonscher A K 1999 Dielectric relaxation in solids *J. Phys. D: Appl. Phys.* **32** 57–70
[37] Hembram K, Rao T N, Srinivasa R S and Kulkarni A R 2015 High performance varistors prepared from doped ZnO nanopowders made by pilot-scale flame spray pyrolyzer: sintering, microstructure and properties *J. Eur. Ceram. Soc.* **35** 3535–44
[38] Tewari S, Ghosh A and Bhattacharjee A 2016 Studies on frequency dependent electrical and dielectric properties of sintered zinc oxide pellets : effects of Al-doping *Indian J. Phys.* **90** 1247–55
[39] Pike G E 1972 ac conductivity of scandium oxide and a new hopping model for conductivity *Phys. Rev.* B **6** 1572–80
[40] Huang D, Liu Z, Li Y and Liu Y 2017 Colossal permittivity and dielectric relaxation of (Li, In) Co-doped ZnO ceramics *J. Alloys Compd.* **698** 200–6
[41] Mccluskey M D 2018 *Defects in Advanced Electronic Materials and Novel Low Dimensional Structures* (Elsevier Ltd) 978-0081020548
[42] Schmidt-mende L and Macmanus-driscoll J L 2007 ZnO - nanostructures, defects, and devices *Mater. Today* **10** 40–8
[43] Janotti A and Van de Walle C G 2009 Fundamentals of zinc oxide as a semiconductor *Rep Prog Phy* **72** 1–29
[44] Ansari S A, Nisar A, Fatma B, Khan W and Naqvi A H 2012 Investigation on structural, optical and dielectric properties of Co doped ZnO nanoparticles synthesized by gel-combustion route *Mater. Sci. Eng.* B **177** 428–35